

## Optimization of Copper and Zinc ions removal from aqueous solution by modified Nano-bentonite using Response surface methodology

Shahab Nasseri<sup>\*1,2,3</sup>, Ali Yagubov<sup>2</sup>, Abdolali Alemi<sup>3</sup>, Ali Nuriev<sup>2</sup>

<sup>1</sup>Technical College of Ibn Sina Khalkhal, Technical and Vocational University, Ardabil, Iran.

<sup>2</sup>Institute of Catalysis and Inorganic Chemistry named after acad. M. F. Nagiyev of Azerbaijan National Academy of Sciences, Baku, Azerbaijan.

<sup>3</sup>Department of Inorganic chemistry, Faculty of chemistry, University of Tabriz, Tabriz, Iran.

Received: 8 July 2018; Accepted: 28 October 2018

\* Corresponding author email: [Naseri1449@gmail.com](mailto:Naseri1449@gmail.com)

### ABSTRACT

In recent decades, the presence of heavy metal ions in wastewater has become an important public concern worldwide. Adsorption is a commonly used technique for removing various types of materials including metal ions from contaminated water sources. However, common methods for adsorption are not completely efficient at low ion concentrations; therefore, adsorbents should be improved in order to reach an acceptable level of adsorption efficiency. In this study, the removal of two heavy metals ions, zinc and copper, from synthetic aqueous solution using Nano-bentonite was investigated. Modified bentonite was obtained by calcination of bentonite at 600 °C for 2h. Response surface methodology (RSM) and central composite design (CCD) were used to optimize the operating factors of the adsorption process. Operation time, adsorbent dosage, ion concentration and pH were the variables and percentage of ion removal was considered as the response. HCl and NaOH were used as chemical agents to adjust pH at optimum level of operating condition for Cu<sup>2+</sup> and Zn<sup>2+</sup> removal which were as follows: Cu<sup>2+</sup> initial concentration: 110.1 mg/L, pH:7.3, time: 96.8 min, adsorbent dosage: 2.1 g/l, and Zn<sup>2+</sup> initial concentration: 105 mg/L, pH: 6.9, time: 73.1 min and adsorbent dosage: 2 g/l. Results and 3D plots exhibited significant proof for accepting the competence of the modified Nano-bentonite as an efficient adsorbent for metals ion removal.

**Keywords:** Response surface methodology, Heavy metal adsorption, Wastewater treatment, Nano bentonite.

### 1. Introduction

Heavy metal ions, such as Fe, Zn, Cu, Co, Ag and Cd, are found in soil as well as in various types of industrial effluents [1, 2]. However, they mostly are found as traces but they can have a significant impact on plants, animals and human life. Presence of heavy metal ions in wastewater is an important public concern. Efficient adsorption of heavy metal ions can be promising solution to partially reduce their various harmful effects. The available methods

for removing heavy metal ions from contaminated water resources including membrane filtration[3], ion exchange resins [4,5], oxidation [6] and precipitation are not completely efficient at low ion concentrations, so adsorption process should be considered as an alternative technique. Adsorption plays a vital role in removing pollutants from water and wastewater resources and it is known as an effective technique [7]. Adsorption has a great potential for treating waste water from color

processing industries, heavy metal contamination or from various other kinds of ions contamination. Adsorption is highly efficient, simple and reusable materials can be applied as adsorbents in the process [8]. In recent years, different categories of potential adsorbents have been assessed for the treatment of heavy metal ions, including fly ash [9], sawdust [10], activated carbon [11], bentonite and kaolinite [12]. Bentonite is a type of clay mainly composed of montmorillonite [13, 14]. It is composed of alumino silicates with the ration of 2:1; one unit of the mentioned structure consists of one  $\text{Al}^{3+}$  octahedral sheet located among two layers of  $\text{Si}^{4+}$  tetrahedral sheet [15]. Bentonite is one of the most widely used substrates as adsorbent for eliminating contaminants from aqueous solutions. It provides many internal and external active sites and has a high surface capacity for ion exchange process. Bentonite efficiency could be dramatically increased by optimization of the operation. Compared to Nano particles, bentonite is a low-cost mineral adsorbent [16], which is widely found in various areas. Although many studies have focused on  $\text{Zn}^{2+}$  and  $\text{Cu}^{2+}$  removal with bentonite, there is still enormous potential to improve the adsorption efficiency of bentonite against the relatively low adsorption capacity of natural clay. Therefore, investigating the removal of mentioned ions using modified bentonite may be helpful.

Response surface methodology, RSM, was first introduced in 1951 by G.E.P. Box and K.B. Wilson. It was applied to a first-degree polynomial equation to model the response variable. RSM is a collection of mathematical and statistical techniques that describe test data obtained from an experiment using linear or square polynomial functions [17]. The main goal of RSM is to investigate response variation by changing the variables to achieve optimized response. Unlike classical experiment designs, RSM reduces the number of experiments as well as the interactive effects of the studied variables. Consequently, materials consumption is decreased accordingly [18].

In the present study, heat-treated bentonite was used as the sorbent for removal of  $\text{Zn}^{2+}$  and  $\text{Cu}^{2+}$  from synthetic aqueous solution. Various parameters were studied to increase the efficiency of heat-treated bentonite in metals ion removal, including time, pH, initial concentration of metal ion and adsorbent dosage. Also, optimization of conditions for selected variables was done by RSM to obtain maximum adsorption percentage.

## 2. Materials and methods

### 2.1. Materials

Zinc and copper salts were purchased from Merck Company (Germany). Bentonite was obtained from the Dash-Salahli deposit of Azerbaijan (Iran). Hydrochloric acid (HCl) and sodium hydroxide (NaOH) were provided from Sigma Aldrich (USA).

### 2.2. Methods

#### 2.2.1. Nano-bentonite preparation

Bentonite is prepared by adding sodium carbonate to natural clay. In order to remove the carbonates and purify the bentonite, the material was subjected to acid treatment using HCl. Adjustments were performed using 0.1 M HCl and 0.1 M NaOH. To increase the physical stability of purchased bentonite, a thermal treatment was also performed at 600°C for 2 h; the calcination temperature was determined by thermo gravimetric analysis [11]. Finally, the prepared bentonite was grinded in a ball mill (MM400 RETSCH) for 10 hours to obtain uniform particle dimensions [11].

#### 2.2.2. Adsorbate solutions

The adsorption study was carried out applying synthetic effluents containing  $\text{Cu}^{2+}$  and  $\text{Zn}^{2+}$  separately. Aqueous solutions were prepared by dissolving  $\text{Cu}(\text{NO}_3)_2 \cdot 4\text{H}_2\text{O}$  and  $\text{Zn}(\text{NO}_3)_2$ , respectively, in deionized water to desired concentrations. Pourbaix diagram was drawn using Hydra Medusa Chemical Diagrams software to determine the predominant chemical species of  $\text{Cu}^{2+}$  and  $\text{Zn}^{2+}$ , and also the isoelectric point or pH of zero charge ( $\text{pH}_{\text{ZPC}}$ ). The pH (MP511 Benchtop pH Meter Kit) was set by applying 0.1 M  $\text{HNO}_3$ . Concentrations of Zinc and copper ions were determined using an atomic absorption spectrophotometer (Perkin Elmer ANALYST-100) [19].

#### 2.2.3. Adsorption process

Batch adsorption experiments were carried out in 100 ml solution containing heavy metal by adding the desired concentrations of modified bentonite. The pH for copper and zinc solutions was 7.3 and 6.9, respectively. The batch solution was stirred using a mechanical mixer in a thermostatic glass bottle at a specified rate. At the end of the adsorption experiment, the solution was centrifuged. The amount of adsorbate removal was determined using a UV-Vis spectrophotometer

(Model AA-6300 SHIMADZU). The adsorption capacity and efficiency of ions removal were calculated using the equations Eq.1, Eq.2 [20]

$$q_t = (C_0 - C_t) \times V / m \quad (1)$$

$$\text{Adsorbate removal (\%)} = (C_0 - C_t) \times 100 / C_0 \quad (2)$$

Where  $q_t$  in Eq. (1) is adsorption capacity (mg/g) at any time,  $V$  is volume (L) and  $m$  is adsorbent dose (g). In the second equation,  $C_0$  and  $C_t$  are concentrations of ion before and after adsorption (mg/L) at various periods of time [20].

#### 2.2.4. Determination of concentration

The determination of heavy metals in their particulate and dissolved forms was done according to the procedure which is reported by Karvelas et al [21]. Determination of heavy metal concentrations (Cu and Zn) included sludge sample preparation, i.e., initial drying for 48 h at room temperature until air-dried and then to constant mass at 105°C. In the next step, sludge samples were milled in a mortar grinder. Afterwards, 0.2 g of sample was digested with nitric acid ( $\text{HNO}_3$ ) and hydrochloric acid (HCl) in a Teflon flask, using a microwave digestion system (Multiwave 3000, Anton Paar GmbH, and Graz, Austria). Obtained solutions were filtered through fine filters (0.45  $\mu\text{m}$ ) and diluted with 5%  $\text{HNO}_3$  to a volume of 50 mL. Samples were stored at 4°C prior to analysis. The heavy metal concentration was determined using the atomic absorption spectrophotometer (AAS) (Model AA-6300 SHIMADZU).

#### 2.2.5. Removal of heavy metals from aqueous solution

The metal solutions of proper concentrations were remade by diluting the reference solution to 1000 ppm. The pH was adjusted via using drops of 1M HCl or 1M NaOH. Adsorption experiments were performed as follows: 0.05 g of adsorbent and 10 ml solution were mixed using a glass stirrer in a flask with thermostatically controlled environment using a thermostat IT-1 up to 0.1°C. Concentrations of  $\text{Cu}^{2+}$  and  $\text{Zn}^{2+}$  ions in solutions were determined spectrometrically using a device SF-26. The adsorption capacity and ions removal efficiency were calculated as follows Eq.1.

For comparison the adsorption capacity, activated charcoal was used. In this study, the removal of cations by Na-bentonite from

wastewater was tested in industrial plants. The water was released from columns containing activated charcoal and Na-bentonite.

### 2.3. Characterization of Nano-bentonite

The natural bentonite and Nano-bentonite were analyzed by X-ray diffraction, FT-IR spectroscopy, differential scanning calorimetric analysis, SEM and DLS analysis.

The XRD patterns of the samples were prepared using the Philips X'PERT X-ray diffractometer tool with filtered Cu K $\alpha$  radiation, at voltage 40 kV, 40 mA, step size of 0.02 and time per step of 1.0 seconds. Spectra were carried out by the (Spectrum D ne- FT-IR, Perkin Elmer). The FT-IR spectra of the samples obtained into KBr pellets were collected in the wave number range of 4000-400  $\text{Cm}^{-1}$ . The differential scanning calorimetric analysis was performed using a Shimadzu thermal analyzer in the following conditions: flow rate of 50 ml/min of  $\text{N}_2$ , heating rate 10°C/min and temperature of 500°C. The surface morphology of the samples was determined by a scanning electron microscope (3200 KYKY\_EM) at an accelerated voltage of 26 KV [22]. The samples were coated with gold for a few seconds to be conductive. Then the surface morphology of bentonite was investigated by SEM. The average size distribution of samples particle was determined by DLS analysis (Malvern Instruments, Malvern, UK) at a scattering angle of 90° and laser light irradiation at 657 nm at 25°C [22].

The bentonite used in this study is high-swelling bentonite and has a bulk density of 600-1000  $\text{kg/m}^3$  (Eq.3), determined according to the procedure described by Ahmedna et al. [23] and Huerta-Pujol et al. [24], and a specific surface area (SSA) of 240  $\text{m}^2/\text{gr}$ , specific surface area measured using EGME method [25].

$$\text{Bulk density (Kg/m}^3\text{)} = \text{Weight of bentonite/Volume} \quad (3)$$

The particle size varies between 100-2,000 nm (0.1-2  $\mu\text{m}$ ). The cation exchange capacity (CEC) of a clay is a measure of the quantity of negatively charged sites on clay surfaces that can retain positively charged ions (cations) such as calcium ( $\text{Ca}^{2+}$ ), magnesium ( $\text{Mg}^{2+}$ ), and potassium ( $\text{K}^+$ ), by electrostatic forces. Cations retained electrostatically are easily exchangeable with cations in the clay solution so a clay with a higher CEC has a greater capacity to maintain adequate quantities of  $\text{Ca}^{2+}$ ,  $\text{Mg}^{2+}$  and  $\text{K}^+$  than a clay with a low CEC.

The efficacy of the methods used in the purification of bentonite was evaluated by estimation of cation exchange capacity [26]. Ammonium acetate method was used to measure the cation exchange capacity of bentonite samples (pH=7)[27]. The results showed that the cation exchange capacity of the primary bentonite sample reached from 105-130 cmol/kg in the purified sample indicating an increase in purity of montmorillonite after purification. The cation exchange capacity of pure montmorillonite is 80-150 cmol/kg [26].

**2.4. Response surface methodology and experimental design**

CCD is a beneficial method for identification of an appropriate model. Five-level CCD with four factors evaluates classic data by using a minimum number of runs and investigates the effects of various types of variables [28]. Totals number of experiments in the CCD includes 2n axial runs, 2<sup>n</sup> factorial runs, n<sub>c</sub> and center runs. In addition n is the Number of independent variables (Eq.4).

$$N = 2^n + 2n + n_c \tag{4}$$

By considering Eq.4, the total number of experiments with 4 variables was 30. It should be mentioned that the center point plays an important role in determining the experimental error. The axial points are located at (±α,0,0), (0,±α,0) and (0,0,±α). The factorial part of the design has a direct relation with choosing the value of α. In this study, α was selected as 2. The independent variables and their values were selected in accordance with the results of classical experiments as reported in Tables 1 and 2.

The mathematical relation between independent

parameters is shown as the second order polynomial equation (Eq. 5).

$$Y = \beta_0 + \sum_{i=1}^k \beta_i x_i + \sum_{i=1}^k \beta_{ii} x_i^2 + \sum_{i=1}^{k-1} \sum_{j=i+1}^k \beta_{ij} x_i x_j \tag{5}$$

Where “Y” is the predicted response (removal percentage); x<sub>i</sub> and x<sub>j</sub> are the known independent variables for each experimental run (pH, time, adsorbent dosage and pollutant dosage), B<sub>0</sub> is the constant, B<sub>i</sub> is the linear coefficient; B<sub>ii</sub> is the quadratic coefficient and B<sub>ij</sub> is the cross-product coefficient. Design expert software (version 7.0.0) was used to enhance the mathematical and analytical model and to estimate the response surfaces.

**2.5. Development of the regression model equation**

Central Composite Designs (CCD) was used to test 5 levels of the test variables: time, pH, adsorbent dosage and pollutant concentration. Factor optimization is one of the most important advantages of this model. Adsorption of copper ions and zinc ions was the response. The CCD method was applied to develop a correlation between adsorption percentage and the variables. Mathematical analysis recommended a quadratic model for adsorption of both the tested ions. Regression analysis was applied for fitting the response of surface occupation of heavy metals adsorption.

**2.6. Optimization using the desirability function**

One of the most desirable points about RSM compared with other methods, is converting the discontinuous universe to a continuous one by a polynomial equation. In the process of optimization, consideration of the target allows

Table 1- Parameters and scope of Cu<sup>2+</sup> removal in CCD

Parameter	factor	Unit	Scope				
			2	1	0	-1	-2
pH	X <sub>1</sub>	---	8.56	7.80	6.95	6.10	5.25
Pollutant Co	X <sub>2</sub>	mg/L	185	148	111	74	37
Adsorbent dosage	X <sub>3</sub>	g/L	3	2.5	2	1.5	1
Time	X <sub>4</sub>	Min	120	90	60	30	20

Table 2- Parameters and scope of Zn<sup>2+</sup> removal in CCD

Parameter	factor	Unit	Scope				
			2	1	0	-1	-2
pH	X <sub>1</sub>	---	8.56	7.80	6.95	6.10	5.25
Pollutant Co	X <sub>2</sub>	mg/L	175	140	105	70	35
Adsorbent dosage	X <sub>3</sub>	g/L	3	2.5	2	1.5	1
Time	X <sub>4</sub>	Min	120	90	60	30	20

determining minimization and maximization of the specified factors [29]. In an optimization process using RSM, the desirability function,  $d_f$ , plays an important role. The desirability function includes a simple mathematical policy to calculate optimized values. As a general rule,  $d_f$  value for each dependent value is determined in the range of 0 to 1. Meanwhile, the desirability value 1 was assigned to maximum removal, 0 was assigned to minimum removal and 0.5 was assigned to the middle point. Scores for individual desirability were used to calculate removal amounts, and desirability of 1.0 was chosen as the target value. In this study, the main goal was to achieve a higher percentage of heavy metal ion removal. Therefore, the selected target value was 90% removal for optimization of heavy metals removal. Furthermore, values of considered variables and factors were studied separately under the mentioned conditions (90% removal) for both metals.

### 3. Results and discussion

#### 3.1. Structural analysis

##### 3.1.1. X-ray diffraction analysis

The XRD results for bentonite and modified bentonite are shown in Fig. 1- a, b. The presence of montmorillonite peak in Fig. 1 confirms that there

is montmorillonite in the studied bentonite and modified bentonite samples.

##### 3.1.2. FTIR spectroscopy analysis

Figs. 2 and 3 show the FTIR spectra of natural bentonite and modified bentonite with sodium cation. As can be seen from the results of FTIR spectroscopy, sodium chloride affects the bentonite structure. In the FTIR spectra of bentonite, the attendance of OH<sup>-</sup> groups expressed through the band at 3646 Cm<sup>-1</sup>. The bands at 2925Cm<sup>-1</sup> and 2855Cm<sup>-1</sup> are due to aliphatic hydrocarbons in the bentonite. The adsorption peaks at 463 cm<sup>-1</sup> and 520 Cm<sup>-1</sup> refer to the presence of quartz (Si-O-Si) and Al-O-Si bending vibrations. Smectite originated are also bands at around 1100, 1000 assigned to Si-O stretching vibrations [30]. In FTIR spectra of Na-bentonite, the obtained absorption bands are corresponded to vibration in water molecules, quartz and calcite. In the FTIR spectra, broad bands around 3644.96 and 1741.65 Cm<sup>-1</sup> are attributed to stretching and bending vibrations, respectively, of OH<sup>-</sup> groups in water molecules. The band at 2926Cm<sup>-1</sup> is due to aliphatic hydrocarbons in the Na-bentonite. The very strong absorption peak at 1066 Cm<sup>-1</sup> is caused by Si-O bending vibration. The bands at 462 and 519 Cm<sup>-1</sup> are assigned to Si-O-Si and Al-O-Si bending vibrations [31].

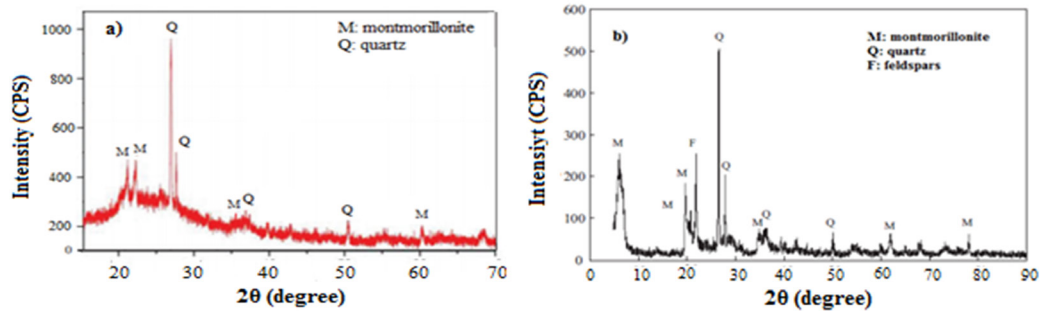


Fig. 1- The XRD patterns of natural bentonite (a) and modified bentonite with sodium (b).

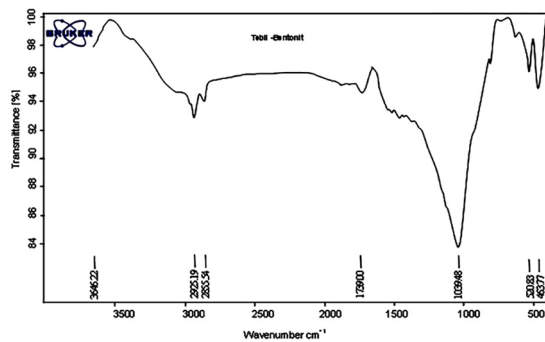


Fig. 2- The FTIR spectra of natural bentonite.

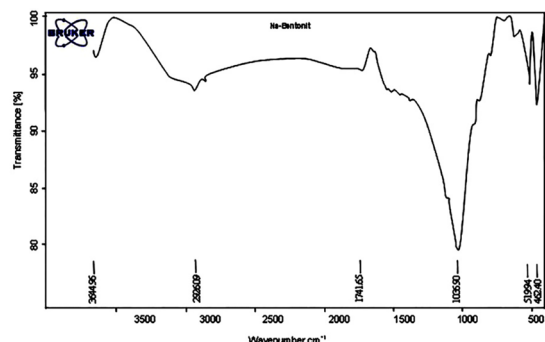


Fig. 3- The FTIR spectra of modified bentonite with sodium cation.

### 3.1.3. Thermal analysis

In Fig. 4, the results of thermal analysis for the bentonite samples are presented. To improve the properties and modify and adjust the chemical composition of bentonite, heat activation is recommended [32, 33].

Heat in various ways, including: alteration of pore water properties and transformation of bentonite particles causes a considerable change in the properties of clays. When bentonite is heated to 150°C, the exchange cations lose their water and their layers come close to each other [34]. This change in the properties of bentonite results in the absorption of more cations by activated bentonite.

In Fig. 4, different thermal effects are observed. The high endothermic peak at 100-120°C is attributed to removal of the surface water and the peak at 500-510°C is related to the removal of water from the bulk. The reason for the peak at 660°C is Hydroxide withdrawal from the montmorillonite network [35].

### 3.2. Morphology Observations

Fig. 5 shows the SEM micrographs of bentonite species. Also Fig. 5 shows that the montmorillonite particles exist in format of large and small leaf shape bowls. The porous micro-structured bentonite samples are created by the accumulation of larger particles. Micro associations have a series of interactions between themselves and make it possible to create porosities in different sizes [36].

According to the DLS analysis particle size distribution was wide and the average size ranged from 70 nm to 280 nm.

### 3.3. Adsorption process

Removal efficiency of  $\text{Cu}^{2+}$  and  $\text{Zn}^{2+}$  were shown in Table 3. As seen in Table 3, the ion removal efficiency increases with raising pH values. These results show that the pH is an important parameter affecting the removal of  $\text{Cu}^{2+}$  and  $\text{Zn}^{2+}$ . Also the adsorption parameters were obtained from the Langmuir and Freundlich equations. The results of this section are summarized in Table 4. From this table we understand that the performance of the Langmuir equation is better than the Freundlich equation, because the  $R^2$  value for Langmuir equation is closer to unit. Clays have a layered structure and have a negative charge. Because of this negative charge, a layer of clay is used as a suitable adsorbent in the removal of heavy metal cations [37, 38]. The adsorption of materials on

the solid adsorbent is due to the force of attraction between the adsorbent and the adsorbent surface. The specific mechanisms and forces that attract the dissolved material to the surface of the adsorbent can be physical or chemical. The adsorption mechanism is essentially that of mass transfer of soluble molecules (metal cations) from the aqueous solution mass to the surface of the Na-bentonite adsorbent, then penetration from the internal structure of the Na-bentonite particles to the adsorption sites and the adsorption process is carried out quickly. The adsorption process occurs so rapidly that no resistance is observed during the adsorption process, so that mass transfer and intra-particle diffusion act as the determinant of the adsorption rate [39].

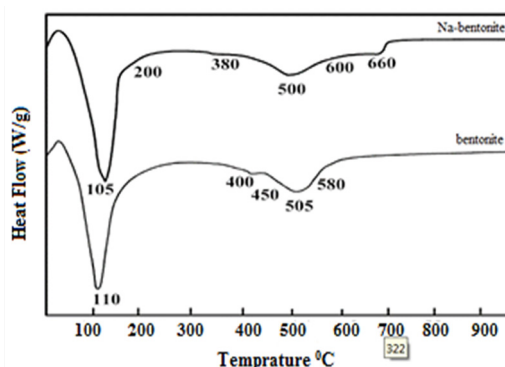


Fig. 4- Thermal analysis for natural bentonite and modified bentonite with sodium.

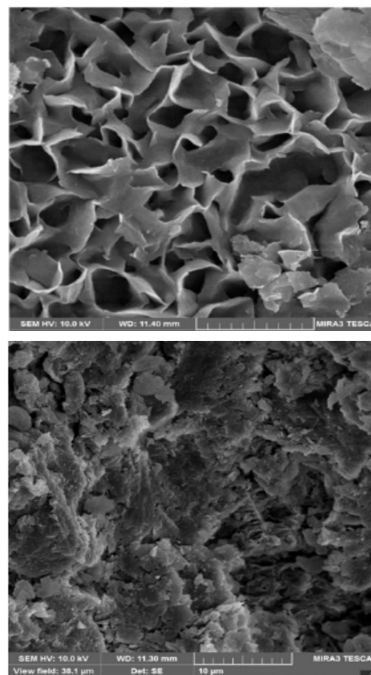


Fig. 5- SEM micrographs of bentonite species.

Table 3- Removal efficiency of Cu<sup>2+</sup> and Zn<sup>2+</sup>

	Initial concentration (ppm)	Remaining concentration in aqueous solution (ppm)	pH	Removal efficiency (%)
Cu <sup>2+</sup>	5.00	0.100	3.00	97.40
		0.229	5.30	95.42
		0.279	7.30	94.42
		1.240	3.00	75.20
Zn <sup>2+</sup>	5.00	2.493	5.30	50.14
		1.477	7.30	70.46

Table 4- Characteristic, parameters and determination coefficient of the experimental data according to the degree of correlation Langmuir and Freundlich

	Langmuir parameters			Freundlich parameters		
	X(mg/g)	b(L/mg)	R <sup>2</sup>	K <sub>F</sub>	n	R <sup>2</sup>
Zn <sup>2+</sup>	18.52	0.092	0.9948	1.485	1.467	0.8461
Cu <sup>2+</sup>	19.92	3.461	0.9948	1.467	1.012	0.9312

### 3.4. Development of the regression model equation

The obtained models for Cu<sup>2+</sup> and Zn<sup>2+</sup> ions are presented as (Eq.6) and (Eq.7) respectively:

$$Y_{Cu} = 81.4983 + 7.0758X_1 - 10.287X_2 + 9.6259X_3 + 6.4521X_4 \quad (6)$$

$$Y_{Zn} = 86.7374 + 9.2079X_1 - 8.1671X_2 - 11.7471X_3 + 7.6110X_4 - 6.9715X_1^2 - 4.7627X_2^2 - 7.3002X_3^2 \quad (7)$$

Where “Y” illustrates adsorption of heavy metal ions. X<sub>1</sub>, X<sub>2</sub>, X<sub>3</sub> and X<sub>4</sub> show pH, pollutant dosage, adsorbent dosage and time, respectively. In these equations, positive or negative signs relating to the different variables indicate the effect of each on the adsorption process. Negative signs specify antagonistic behavior and positive signs indicate synergistic behavior.

### 3.5. Response surface methodology

In order to optimize the critical factors in the process of heavy metals ion removal (Cu<sup>2+</sup> and Zn<sup>2+</sup>) the experiments were performed by actions the chosen adsorbent, RSM and CCD. According to the Figs. 6 and 7, which represent the response surface plots of ion removal (%) versus variable, the response surface was an appropriate fit to the design. These plots show values for pairs of variables at the entry values of the others and arches of mapped interactions between the variables.

The percentages of Cu<sup>2+</sup> and Zn<sup>2+</sup> removal illustrate a significant positive relation with adsorbent dosage. The interaction of adsorbent

dosage with other variables illustrates a noticeable relation between the rate of heavy metals removal and adsorbent dosage. The transfer of adsorbate molecules onto the wide surface of the adsorbent led to a higher rate of adsorption. A higher removal rate was observed in the case of Cu<sup>2+</sup> by increasing the adsorbent dosage; this means that removal percentage increased at a higher proportion of adsorbent dose because of the higher content of adsorbent site. In addition, Figs. 8 and 9 present the effect of pollutant concentration on removal percentage. The percentages of Cu<sup>2+</sup> and Zn<sup>2+</sup> removal had a significant negative relation with concentration of heavy metal ion. The rapid and fast transfer of Cu<sup>2+</sup> and Zn<sup>2+</sup> ions to the bentonite adsorbent led to a rapid occupation of the acceptor sites. The results demonstrate that by increasing the concentration of the pollutant, there was a rapid initial adsorption rate due to the affinity of ions to the vacant sites and then the driving force caused a decrease in removal percentage relation to the additional ions. The interaction of pH with the other variables and adsorbent dosages is also presented in Figs. 6 and 7. The 3D graphs depict significant efficiency of pH on removal percentage. At the first test, Cu<sup>2+</sup> and Zn<sup>2+</sup> ions removal was gradually improved by increasing the pH value. This phenomenon can be attributed to interaction of the surface charge of adsorbent and its available sites with heavy metal ions at higher pH [40-42]. The results show that the initial adsorption rate remained relatively constant. Meanwhile, the variable of time was less effective on the adsorption process.

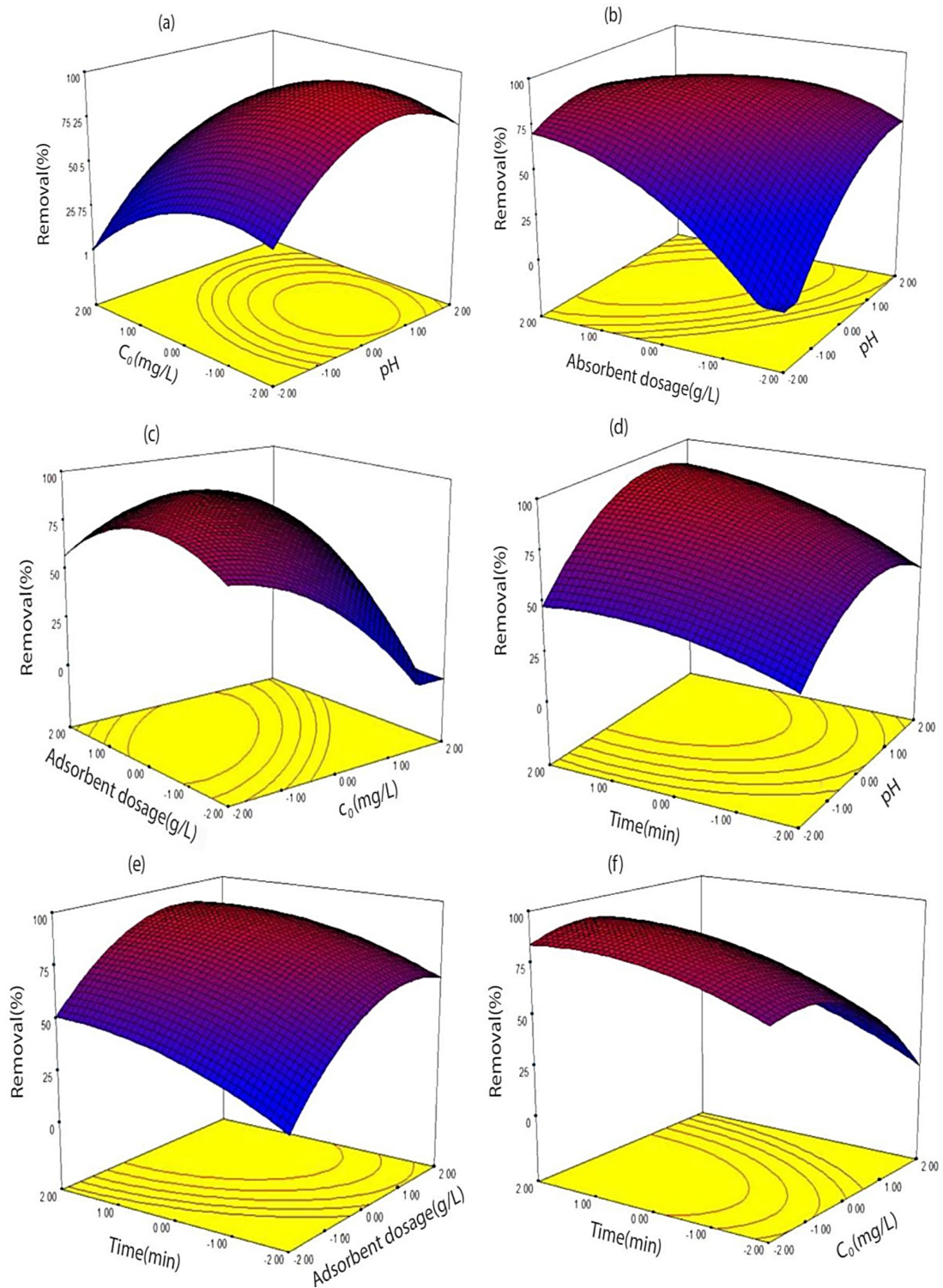


Fig. 6- Results of  $\text{Cu}^{2+}$  removal in response surface for the CCD: (a)  $C_0$ -pH, (b) adsorbent dosage-pH, (c) adsorbent dosage- $C_0$ , (d) Time-pH, (e) Time-adsorbent dosage and (f) Time- $C_0$ .



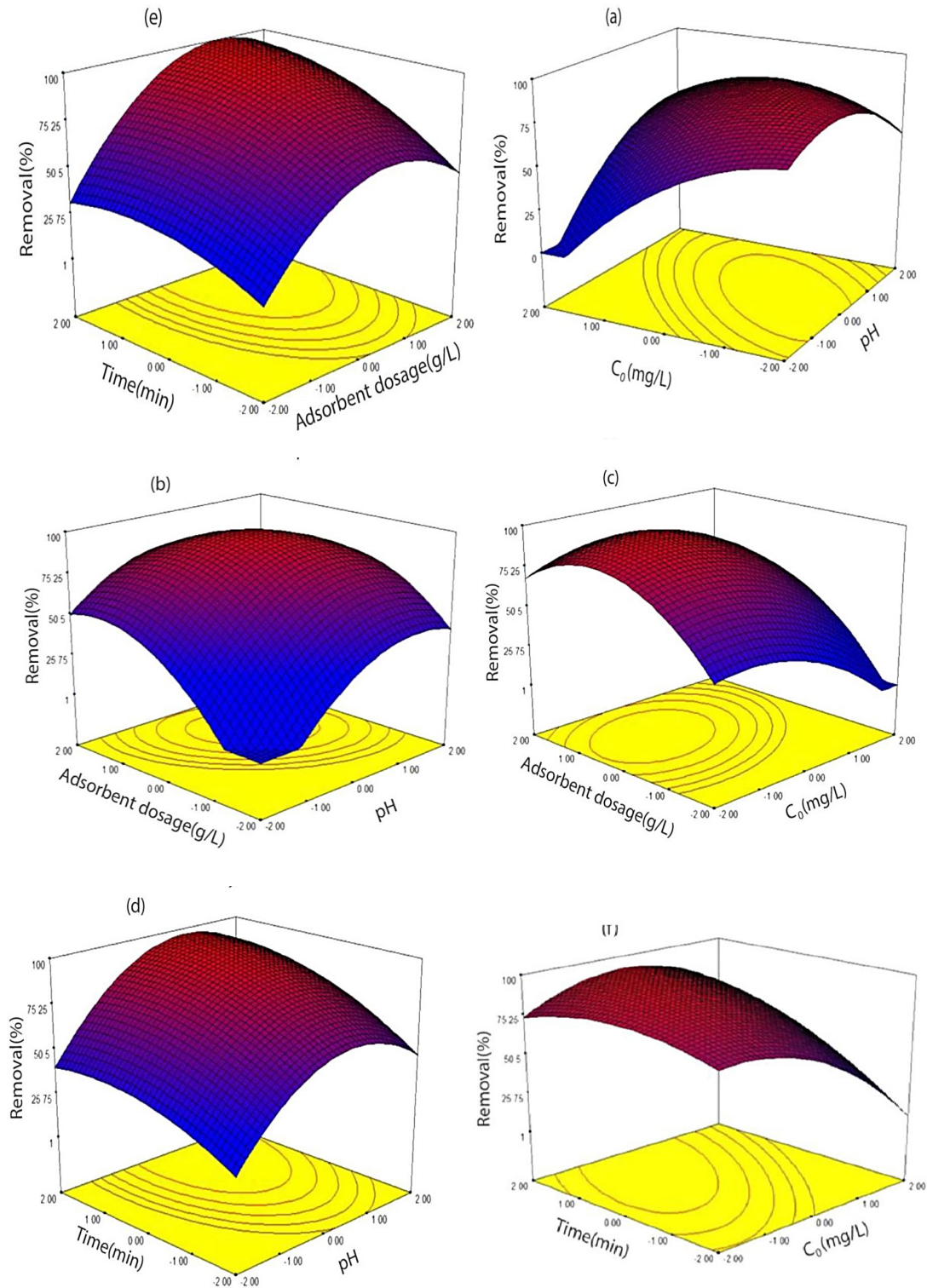


Fig. 7- Results of Zn<sup>2+</sup> (removal in response surface for the CCD: (a) C<sub>0</sub>-pH, (b) adsorbent dosage-pH, (c) adsorbent dosage-C<sub>0</sub>, (d) Time-pH, (e) Time-adsorbent dosage and (f) Time-C<sub>0</sub>.)

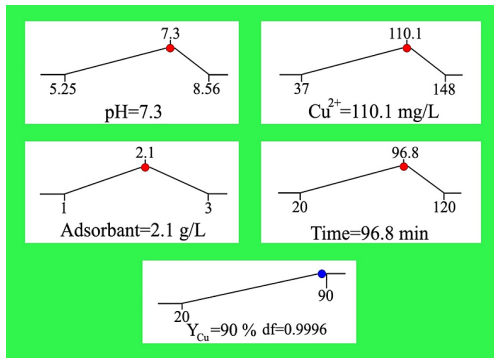


Fig. 8- Predicted optimum condition for Cu<sup>2+</sup> removal.

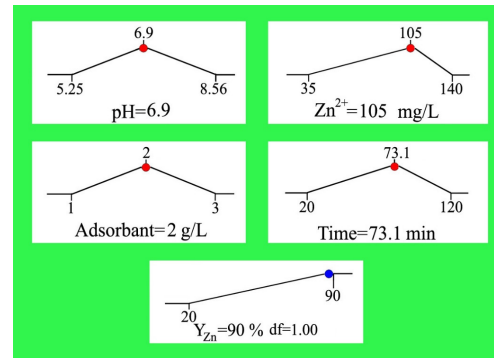


Fig. 9- Predicted optimum condition for Zn<sup>2+</sup> removal.

Table 5- Analysis of variance, ANOVA, for response of the surface model of Cu<sup>2+</sup>

Source	Coe f.	SE Coe f	F-value	P-value
constant	81.4983	4.964	16.416	<0.0001
X <sub>1</sub>	7.0758	2.710	2.611	0.019
X <sub>2</sub>	10.2876	2.710	-3.796	0.002
X <sub>3</sub>	9.6259	2.710	3.552	0.003
X <sub>4</sub>	6.4521	2.798	2.306	0.035
X <sub>1</sub> <sup>2</sup>	-4.9277	2.467	-1.997	0.063
X <sub>2</sub> <sup>2</sup>	-4.9852	2.467	-2.021	0.06
X <sub>3</sub> <sup>2</sup>	-4.8065	2.467	-1.948	0.069
X <sub>4</sub> <sup>2</sup>	-2.1037	2.467	-0.853	0.406
X <sub>1</sub> X <sub>2</sub>	5.9663	3.332	1.791	0.092
X <sub>1</sub> X <sub>3</sub>	-5.7951	3.332	-1.739	0.101
X <sub>1</sub> X <sub>4</sub>	1.6294	3.491	0.467	0.647
X <sub>2</sub> X <sub>3</sub>	6.1799	3.332	1.855	0.082
X <sub>2</sub> X <sub>4</sub>	1.3044	3.491	0.374	0.714
X <sub>3</sub> X <sub>4</sub>	-0.9732	3.491	-0.279	0.784

Table 6- Analysis of variance, ANOVA, for response of the surface model of Zn<sup>2+</sup>

Source	Coe f	SE Coe f	F-value	P-value
constant	86.7374	4.284	20.246	<0.0001
X <sub>1</sub>	9.2079	2.338	3.938	0.001
X <sub>2</sub>	-8.1671	2.338	-3.492	0.003
X <sub>3</sub>	11.7471	2.338	5.023	<0.0001
X <sub>4</sub>	7.611	2.414	3.153	0.006
X <sub>1</sub> <sup>2</sup>	-6.9715	2.129	-3.275	0.005
X <sub>2</sub> <sup>2</sup>	-4.7627	2.129	-2.237	0.04
X <sub>3</sub> <sup>2</sup>	-7.3002	2.129	-3.429	0.003
X <sub>4</sub> <sup>2</sup>	-2.4755	2.129	-1.163	0.262
X <sub>1</sub> X <sub>2</sub>	0.7294	2.875	0.254	0.803
X <sub>1</sub> X <sub>3</sub>	-4.6294	2.875	-1.61	0.127
X <sub>1</sub> X <sub>4</sub>	1.056	3.013	0.351	0.731
X <sub>2</sub> X <sub>3</sub>	2.2744	2.875	0.791	0.441
X <sub>2</sub> X <sub>4</sub>	3.9398	3.013	1.308	0.209
X <sub>3</sub> X <sub>4</sub>	1.9102	3.013	0.634	0.53

### 3.6. CCD statistical analysis

Tables 5 and 6 show analysis of CCD responses and results of ANOVA applied to adsorption study of the heavy metals (Cu<sup>2+</sup> and Zn<sup>2+</sup> ions). Qualification and adequacy were evaluated by analysis of variance which was highly critical. The p-value, which is reported in Table 5, illustrates the significance of each variable and its relation with other variables. As demonstrated in the table, X<sub>1</sub>, X<sub>2</sub>, X<sub>3</sub> and X<sub>4</sub> were significant for Cu<sup>2+</sup> adsorption. Meanwhile, the mentioned variables showed very small P-value (P<0.05). However, their P-value was non-significant for the other variables. Table 6 depicts the significance of each variable for Zn<sup>2+</sup> removal by p-value. By considering the results, all X<sub>1</sub>, X<sub>2</sub>, X<sub>3</sub>, X<sub>4</sub>, X<sub>1</sub><sup>2</sup>, X<sub>2</sub><sup>2</sup> and X<sub>3</sub><sup>2</sup> are known as significant terms in the case of Zn<sup>2+</sup> adsorption; however, X<sub>1</sub>X<sub>2</sub>, X<sub>1</sub>X<sub>3</sub>, X<sub>1</sub>X<sub>4</sub>, X<sub>2</sub>X<sub>3</sub>, X<sub>2</sub>X<sub>4</sub>, X<sub>3</sub>X<sub>4</sub> and X<sub>4</sub><sup>2</sup> are indicated as non-significance terms.

### 3.7. Optimization using the desirability function

Fig. 8 illustrates the results of Cu<sup>2+</sup> removal under specified conditions. D f value was 0.9996 in the case of Cu<sup>2+</sup>, which shows satisfied assessment. On the basis of these calculations, a desirability score of 1.0 (90% removal) was obtained at optimum conditions set as: 96.8 min of contact time, 2.1 g/L of adsorbent dosage at pH of 7.3 and initial Cu<sup>2+</sup> concentration of 110.1 mg/L.

Fig. 9 shows the results of Zn<sup>2+</sup> removal that represent high d f value (d f=1), also by using these conditions, the maximum zinc ions removal efficiency was achieved at 73.1 min contact time, 2 g/L adsorbent dosage, pH 6.9 and initial Zn<sup>2+</sup> concentration of 105 mg/L. These results show conformity of the model with the experimental removal efficiency of the tested heavy metals.

Table 7 demonstrates the optimized values for removal of each metal. It should be mentioned that metal ions removal experiments in optimum

conditions was accomplished three times in order to examine accuracy of model. The results of Cu<sup>2+</sup> and Zn<sup>2+</sup> removal indicated error at 2.04% and 3.33%, respectively. These points represent aptness and accuracy of the model.

**3.8. Development of the regression model equation**

Tables 8 and 9 illustrate the matrix and the results of CCD for Cu<sup>2+</sup> and Zn<sup>2+</sup> ions. As seen in Tables 8 and 9, the maximum removal of copper and zinc ions is occurred in Run 15 ({X<sub>1</sub>=0, X<sub>2</sub>=0, X<sub>3</sub>=2 and X<sub>4</sub>=0} and { X<sub>1</sub>=2, X<sub>2</sub>=0, X<sub>3</sub>=0 and X<sub>4</sub>=0} for zinc ions), respect.

The values of coefficients which were expressed

by CCD method (R<sup>2</sup> ≈ 0.80 for Cu<sup>2+</sup> and R<sup>2</sup> ≈ 0.85 for Zn<sup>2+</sup>), admitted acceptable quality of the mentioned polynomial model as shown in the Fig. 10.

**4. Conclusion**

In this study, statistical methodology and CCD were applied determining optimal conditions for heavy metals adsorption by the modified bentonite. For comparison the adsorption capacity, activated charcoal was used. The results showed that, adsorption capacity of Na-bentonite was 1.5 times higher than that of natural bentonite and activated charcoal. The removal rate of zinc and copper cations was 60-65% in the column containing activated charcoal, while in the

Table 7- Optimized values of variables for heavy metal ions (Cu<sup>2+</sup> and Zn<sup>2+</sup>)

	Initial pH	C <sub>0</sub> (mg/L)	Adsorbent (g/L)	Time (min)	Efficiency (%)	
					predicted	Experimented
Cu <sup>2+</sup>	7.3	110.1	2	96.8	91.0	88.2
Zn <sup>2+</sup>	6.9	105	2.1	73.1	91.0	87.1

Table 8- Experiment design matrix and response results for Cu<sup>2+</sup>

Run	X <sub>1</sub>	X <sub>2</sub>	X <sub>3</sub>	X <sub>4</sub>	Removal(%)
1	0	0	0	0	88.49
2	0	0	0	0	84.68
3	2	0	0	0	100
4	0	0	0	0	86.06
5	1	-1	-1	1	72.89
6	1	1	1	-1	59.07
7	0	0	0	0	88.83
8	-1	-1	-1	-1	45.37
9	-1	-1	1	1	84.5
10	1	-1	1	-1	64.16
11	0	0	-2	0	32.76
12	0	0	0	-2	72.68
13	0	2	0	0	48.09
14	-1	1	1	-1	50.27
15	0	0	2	0	95.03
16	1	-1	1	1	80.66
17	-1	1	1	1	76.66
18	1	-1	-1	-1	71.07
19	0	-2	0	0	100
20	0	0	0	0	88.14
21	0	0	0	0	85.53
22	-1	-1	1	-1	70.12
23	-1	1	-1	-1	29.92
24	-2	0	0	0	30.42
25	0	0	0	2	94.46
26	1	1	1	1	85.59
27	1	1	-1	1	68.51
28	1	1	-1	-1	35.35
29	-1	1	-1	1	42.92
30	-1	-1	-1	1	51.66

Table 9- Experiment design matrix and response results for Zn<sup>2+</sup>

Run	X <sub>1</sub>	X <sub>2</sub>	X <sub>3</sub>	X <sub>4</sub>	Removal(%)
1	0	0	0	0	80.92
2	0	0	0	0	81.64
3	-1	-1	-1	-1	50.36
4	1	1	1	1	89.35
5	0	0	0	-2	65.45
6	1	-1	1	-1	50.78
7	0	0	0	0	81.77
8	0	0	0	0	81.99
9	1	-1	1	1	61.52
10	0	2	0	0	34.59
11	-1	1	1	-1	56.42
12	0	0	-2	0	36.75
13	0	-2	0	0	94.98
14	1	1	-1	-1	37.66
15	2	0	0	0	100
16	0	0	0	2	88.74
17	-1	-1	-1	1	74.05
18	-2	0	0	0	30.03
19	-1	-1	1	-1	83.85
20	0	0	0	0	80.12
21	-1	1	1	1	64.78
22	0	1	-1	1	37.72
23	-1	0	0	0	81.39
24	-1	-1	1	1	91.47
25	0	1	1	-1	63.89
26	-1	1	-1	-1	30.46
27	1	-1	-1	-1	73.8
28	1	1	-1	1	61.15
29	0	0	2	0	94.25
30	1	-1	-1	1	81.28

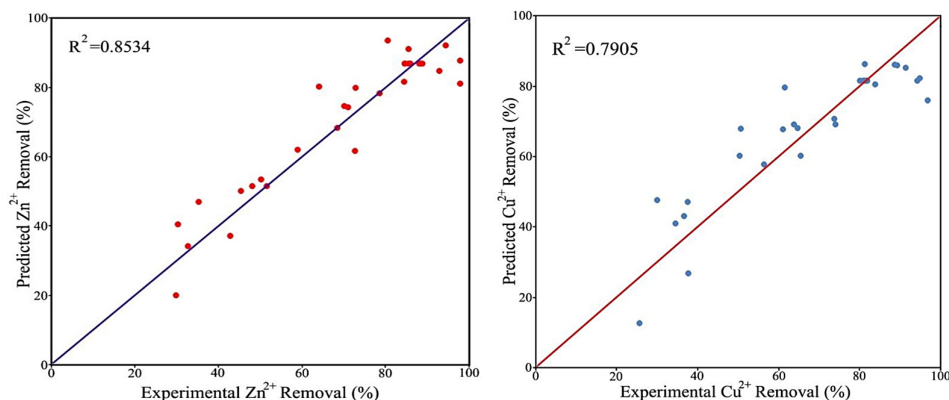


Fig. 10- The experiment removal data versus the predicted data of  $\text{Cu}^{2+}$  and  $\text{Zn}^{2+}$ .

column containing Na-bentonite it was 90-95%. Response surface plots were used to investigate the interactive effects of the variables (initial concentration of metal ions, pH, adsorption time and adsorbent dosage) on the response (heavy metal ion removal). Next, examination by regression analysis of the experimental data was attained from 30 runs. By considering the desirability function, optimization of factors determined the following conditions for  $\text{Cu}^{2+}$ :

initial concentration 110.1 mg/L, pH 7.3, time 96.8 min and adsorbent dosage 2.1g/L, for  $\text{Zn}^{2+}$ : initial concentration 105 mg/L, pH 6.9, time 73.1 min and adsorbent dosage 2g/L. Under optimized conditions, the  $\text{Cu}^{2+}$  and  $\text{Zn}^{2+}$  removal efficiency of 88.2 % and 87.1% with desirability of 0.9996 and 1, were obtained respectively. On the basis of these test results, it appeared that modified bentonite could be a highly efficient substrate for adsorption of pollutants such as heavy metals.

### References

1. Wang J, Ma H, Yuan W, He W, Wang S, You J. Synthesis and characterization of an inorganic/organic-modified bentonite and its application in methyl orange water treatment. *Desalination and Water Treatment*. 2013;52(40-42):7660-72.
2. Wada K. Selective Adsorption of Zinc on Halloysite. *Clays and Clay Minerals*. 1980;28(5):321-7.
3. Fu F, Wang Q. Removal of heavy metal ions from wastewaters: A review. *Journal of Environmental Management*. 2011;92(3):407-18.
4. Dabrowski A, Hubicki Z, Podkościelny P, Robens E. Selective removal of the heavy metal ions from waters and industrial wastewaters by ion-exchange method. *Chemosphere*. 2004;56(2):91-106.
5. Siu PCC, Koong LF, Saleem J, Barford J, McKay G. Equilibrium and kinetics of copper ions removal from wastewater by ion exchange. *Chinese Journal of Chemical Engineering*. 2016;24(1):94-100.
6. Chen J, Wang Y, Ding S, Ding J, Li M, Zhang C, et al. Sub- and super-critical water oxidation of wastewater containing organic and heavy metallic pollutants and recovery of superfine metallic particles. *Journal of Environmental Chemical Engineering*. 2016;4(3):2698-705.
7. Edo J. Adsorption of toxic metals and control of mosquito-borne disease by *Lysinibacillus sphaericus*: dual Benefits for health and environment. *Biomedical and Environmental Sciences*. 2016 Mar 1;29(3):187-96.
8. Kiani G. High removal capacity of silver ions from aqueous solution onto Halloysite nanotubes. *Applied Clay Science*. 2014;90:159-64.
9. Gupta GS, Prasad G, Singh VN. Removal of chrome dye from aqueous solutions by mixed adsorbents: Fly ash and coal. *Water*

10. Kalavathy M H, Regupathi I, Pillai MG, Miranda LR. Modelling, analysis and optimization of adsorption parameters for  $\text{H}_3\text{PO}_4$  activated rubber wood sawdust using response surface methodology (RSM). *Colloids and Surfaces B: Biointerfaces*. 2009;70(1):35-45.
11. Ali RM, Hamad HA, Hussein MM, Malash GF. Potential of using green adsorbent of heavy metal removal from aqueous solutions: Adsorption kinetics, isotherm, thermodynamic, mechanism and economic analysis. *Ecological Engineering*. 2016;91:317-32.
12. Bouberka Z, Kacha S, Kameche M, Elmaleh S, Derriche Z. Sorption study of an acid dye from an aqueous solutions using modified clays. *Journal of Hazardous Materials*. 2005;119(1-3):117-24.
13. Manohar DM, Noeline BF, Anirudhan TS. Adsorption performance of Al-pillared bentonite clay for the removal of cobalt(II) from aqueous phase. *Applied Clay Science*. 2006;31(3-4):194-206.
14. Li Q, Yue Q-Y, Su Y, Gao B-Y, Sun H-J. Equilibrium, thermodynamics and process design to minimize adsorbent amount for the adsorption of acid dyes onto cationic polymer-loaded bentonite. *Chemical Engineering Journal*. 2010;158(3):489-97.
15. Tahir S, Naseem R. Removal of Cr(III) from tannery wastewater by adsorption onto bentonite clay. *Separation and Purification Technology*. 2007;53(3):312-21.
16. Anirudhan TS, Ramachandran M. Adsorptive removal of tannin from aqueous solutions by cationic surfactant-modified bentonite clay. *Journal of Colloid and Interface Science*. 2006;299(1):116-24.

17. Iqbal M, Iqbal N, Bhatti IA, Ahmad N, Zahid M. Response surface methodology application in optimization of cadmium adsorption by shoe waste: A good option of waste mitigation by waste. *Ecological Engineering*. 2016;88:265-75.
18. Bezerra MA, Santelli RE, Oliveira EP, Villar LS, Escalera LA. Response surface methodology (RSM) as a tool for optimization in analytical chemistry. *Talanta*. 2008;76(5):965-77.
19. Han W, Fu F, Cheng Z, Tang B, Wu S. Studies on the optimum conditions using acid-washed zero-valent iron/aluminum mixtures in permeable reactive barriers for the removal of different heavy metal ions from wastewater. *Journal of Hazardous Materials*. 2016;302:437-46.
20. Desta MB. Batch sorption experiments: Langmuir and Freundlich isotherm studies for the adsorption of textile metal ions onto teff straw (*Eragrostis tef*) agricultural waste. *Journal of thermodynamics*. 2013;2013.
21. Karvelas M, Katsoyiannis A, Samara C. Occurrence and fate of heavy metals in the wastewater treatment process. *Chemosphere*. 2003;53(10):1201-10.
22. Jahanizadeh S, Yazdian F, Marjani A, Omidi M, Rashedi H. Curcumin-loaded chitosan/carboxymethyl starch/montmorillonite bio-nanocomposite for reduction of dental bacterial biofilm formation. *International Journal of Biological Macromolecules*. 2017;105:757-63.
23. Brigatti MF, Galan E, Theng BKG. Chapter 2 Structures and Mineralogy of Clay Minerals. *Developments in Clay Science*: Elsevier; 2006. p. 19-86.
24. Ahmedna M, Johns MM, Clarke SJ, Marshall WE, Rao RM. Potential of agricultural by-product-based activated carbons for use in raw sugar decolourisation. *Journal of the Science of Food and Agriculture*. 1997;75(1):117-24.
25. Huerta-Pujol O, Soliva M, Martínez-Farré FX, Valero J, López M. Bulk density determination as a simple and complementary tool in composting process control. *Bioresource Technology*. 2010;101(3):995-1001.
26. Eltantawy IM, Arnold PW. REAPPRAISAL OF ETHYLENE GLYCOL MONO-ETHYL ETHER (EGME) METHOD FOR SURFACE AREA ESTIMATIONS OF CLAYS. *Journal of Soil Science*. 1973;24(2):232-8.
27. Thuc C-NH, Grillet A-C, Reinert L, Ohashi F, Thuc HH, Duclaux L. Separation and purification of montmorillonite and polyethylene oxide modified montmorillonite from Vietnamese bentonites. *Applied Clay Science*. 2010;49(3):229-38.
28. Singh S, Ma L, Hendry M. Characterization of aqueous lead removal by phosphatic clay: Equilibrium and kinetic studies. *Journal of Hazardous Materials*. 2006;136(3):654-62.
29. Nurchi VM, Crisponi G, Villaescusa I. Chemical equilibria in wastewaters during toxic metal ion removal by agricultural biomass. *Coordination Chemistry Reviews*. 2010;254(17-18):2181-92.
30. Benguella B, Yacouta-Nour A. Adsorption of Bezanyl Red and Nylomine Green from aqueous solutions by natural and acid-activated bentonite. *Desalination*. 2009;235(1-3):276-92.
31. Atia A. Adsorption of chromate and molybdate by cetylpyridinium bentonite. *Applied Clay Science*. 2008;41(1-2):73-84.
32. Malkoc E, Nuhoglu Y. Potential of tea factory waste for chromium(VI) removal from aqueous solutions: Thermodynamic and kinetic studies. *Separation and Purification Technology*. 2007;54(3):291-8.
33. Zhu B, Fan T, Zhang D. Adsorption of copper ions from aqueous solution by citric acid modified soybean straw. *Journal of Hazardous Materials*. 2008;153(1-2):300-8.
34. Phillips M, Cataneo RN, Cummin ARC, Gagliardi AJ, Gleeson K, Greenberg J, et al. Detection of Lung Cancer With Volatile Markers in the Breatha. *Chest*. 2003;123(6):2115-23.
35. Baysal Z, Çınar E, Bulut Y, Alkan H, Dogru M. Equilibrium and thermodynamic studies on biosorption of Pb(II) onto *Candida albicans* biomass. *Journal of Hazardous Materials*. 2009;161(1):62-7.
36. Said KA, Amin MA. Overview on the response surface methodology (RSM) in extraction processes. *Journal of Applied Science & Process Engineering*. 2015;2(1).
37. Ahmadi S, Bazrafshan E, Kord Mostafapoor F. Treatment of landfill leachate using a combined Coagulation and modify bentonite adsorption processes. *J Sci Eng Res*. 2017;4(2):58-64.
38. Amarasinghe BMWPK, Williams RA. Tea waste as a low cost adsorbent for the removal of Cu and Pb from wastewater. *Chemical Engineering Journal*. 2007;132(1-3):299-309.
39. Ramavandi B, Asgari G, Faradmal J, Sahebi S, Roshani B. Abatement of Cr (VI) from wastewater using a new adsorbent, cantaloupe peel: Taguchi L16 orthogonal array optimization. *Korean Journal of Chemical Engineering*. 2014;31(12):2207-14.
40. Mouni L, Merabet D, Bouzaza A, Belkhir L. Adsorption of Pb(II) from aqueous solutions using activated carbon developed from Apricot stone. *Desalination*. 2011;276(1-3):148-53.
41. Alghamdi AA, Al-Odayni A-B, Saeed WS, Al-Kahtani A, Alharthi FA, Aouak T. Efficient Adsorption of Lead (II) from Aqueous Phase Solutions Using Polypyrrole-Based Activated Carbon. *Materials*. 2019;12(12):2020.
42. Uddin MK. A review on the adsorption of heavy metals by clay minerals, with special focus on the past decade. *Chemical Engineering Journal*. 2017;308:438-62.